Multiple PPR protein interactions are involved in the RNA editing system in *Arabidopsis* mitochondria and plastids

Nuria Andrés-Colás[a], Qiang Zhu[a,1], Mizuki Takenaka[b], Bert De Rybel[c,d,e], Dolf Weijers[c], and Dominique Van Der Straeten[a,2]

[a]Laboratory of Functional Plant Biology, Department of Biology, Ghent University, B-9000 Gent, Belgium; [b]Molekulare Botanik, Universitaet Ulm, D-89069 Ulm, Germany; [c]Laboratory of Biochemistry, Wageningen University and Research, 6708 WE Wageningen, The Netherlands; [d]Department of Plant Biotechnology and Bioinformatics, Ghent University, 9052 Ghent, Belgium; and [e]Center for Plant Systems Biology, Vlaams Instituut voor Biotechnologie, 9052 Ghent, Belgium

Edited by Robert Haselkorn, University of Chicago, Chicago, IL, and approved June 29, 2017 (received for review April 7, 2017)

Recent identification of several different types of RNA editing factors in plant organelles suggests complex RNA editosomes within which each factor has a different task. However, the precise protein interactions between the different editing factors are still poorly understood. In this paper, we show that the E$^+$-type pentatricopeptide repeat (PPR) protein SLO2, which lacks a C-terminal cytidine deaminase-like DYW domain, interacts in vivo with the DYW-type PPR protein DYW2 and the P-type PPR protein NUWA in mitochondria, and that the latter enhances the interaction of the former ones. These results may reflect a protein scaffold or complex stabilization role of NUWA between E$^+$-type PPR and DYW2 proteins. Interestingly, DYW2 and NUWA also interact in chloroplasts, and DYW2-GFP overexpressing lines show broad editing defects in both organelles, with predominant specificity for sites edited by E$^+$-type PPR proteins. The latter suggests a coordinated regulation of organellar multiple site editing through DYW2, which probably provides the deaminase activity to E$^+$ editosomes.

SLO2 | DYW2 | NUWA | PPR | RNA editing

The PPR family is classified into the P and PLS subfamilies, depending on the PPR signature domains. The P subfamily was described to participate in RNA stabilization, cleavage, splicing, and translation (1). Their members can bind specific RNA sequences to protect them from endonucleases or modify their secondary structure to recruit other RNA maturation factors (2). The P-type PPR protein PPME was the first one described with a role in RNA editing via RNA binding (3). The PLS subfamily is further divided into PLS, E, E$^+$, and DYW subgroups, based on the C-terminal extensions and plays a major role in C-to-U RNA editing in plant organelles. Among them, E and E$^+$-type PPR proteins do not have the DYW domain, which is considered to be a part of the catalytic domain due to the similarity to cytidine deaminase (2), suggesting the requirement of forming protein complexes with a DYW protein for a complete editing event. Indeed, the E-type PPR protein CRR4 forms a complex with DYW1, which consists of only a DYW domain, to edit an ndhD site in chloroplasts (4). However, such transassociated DYW-type PPR protein in an editing complex was reported only at this site in chloroplasts. It is still unclear whether this scenario is universal for numerous RNA editing sites in plant mitochondria. Not only the composition but the stoichiometry of the proteins in the editosome complexes remains unsolved (5). Some PPR proteins can homodimerize to bind RNA, although dimerization can also occur in the absence of the RNA target (6).

Most of the PPR proteins are located in mitochondria (65%) or chloroplasts (17%) (7). Systematic localization experiments and data integration showed that PPR dual targeting occurs more frequently than expected (7, 8). Interestingly, some heat shock proteins (HSPs) have also been associated with editing processes, translocating the editing factors into the required organelle (9).

Previously, we characterized the mitochondrial E$^+$-type PPR protein SLO2, which participates in the editing of *mttB*-144, *mttB*-145, *nad4L*-110, *nad7*-739, *mttB*-666, *nad1*-2, and *nad1*-40 sites, affecting four proteins of complex I in the mitochondrial electron transport chain (10). However, SLO2 lacks a catalytic domain responsible for the editing task. In this report, we aimed to elucidate which proteins participate in the working mechanism of SLO2 by identifying its interacting partners.

Results

Immunoprecipitation with SLO2 Reveals PPR- and HSP-Type Candidate Interactors. As a first approach to identify interacting partners of the E$^+$-type PPR protein SLO2, we performed an immunoprecipitation and mass spectrometry (IP–MS) assay. Total protein extracts from *Arabidopsis* seedlings expressing a green fluorescent protein (GFP)-tagged SLO2 protein (SLO2-GFP), either under control of the *SLO2* or the CaMV *35S* promoter, were taken as starting material. Among the top 25 interactors, after selection of significant data (P value <0.05) and sorting based on the ratio of *pSLO2::SLO2* to the Col-0 wild-type control (Fig. S1), three types of proteins were chosen: PPR proteins with a DYW domain (DYW2-At2g15690 and MEF57-At5g44230), P-type PPR proteins

Significance

RNA editing is a posttranscriptional regulation process essential for organellar function. The PPR protein family plays a major role in RNA editing, but the precise function of each member and its interactions in editosome complexes remain unclear. This research demonstrates that three PPR proteins (SLO2, NUWA, and DYW2) interact in mitochondria and provides evidence for the following: (*i*) P-type PPR protein NUWA assists in the interaction between SLO2 and DYW2, and (*ii*) DYW2 participates in E$^+$ editosomes. We hypothesize that this mechanism is common in both mitochondria and chloroplasts, where the E$^+$-type PPR proteins, such as SLO2, target the specific RNA sites, with DYW2 suggested to provide the editing catalytic domain and NUWA assisting the interaction between the former ones.

Author contributions: N.A.-C., Q.Z., and D.V.D.S. designed research; N.A.-C., Q.Z., M.T., and B.D.R. performed research; N.A.-C., Q.Z., M.T., B.D.R., D.W., and D.V.D.S. analyzed data; Q.Z., M.T., B.D.R., and D.W. revised and commented on the draft manuscript; D.V.D.S. coordinated the project; and N.A.-C. and D.V.D.S. wrote the paper.

The authors declare no conflict of interest.

This article is a PNAS Direct Submission.

[1]Present address: Basic Forestry and Proteomics Center, Fujian Provincial Key Laboratory of Haixia Applied Plant Systems Biology, Haixia Institute of Science and Technology, Fujian Agriculture and Forestry University, 350002, Fujian, China.

[2]To whom correspondence should be addressed. Email: dominique.vanderstraeten@ugent.be.

This article contains supporting information online at www.pnas.org/lookup/suppl/doi:10.1073/pnas.1705815114/-/DCSupplemental.

PLANT BIOLOGY

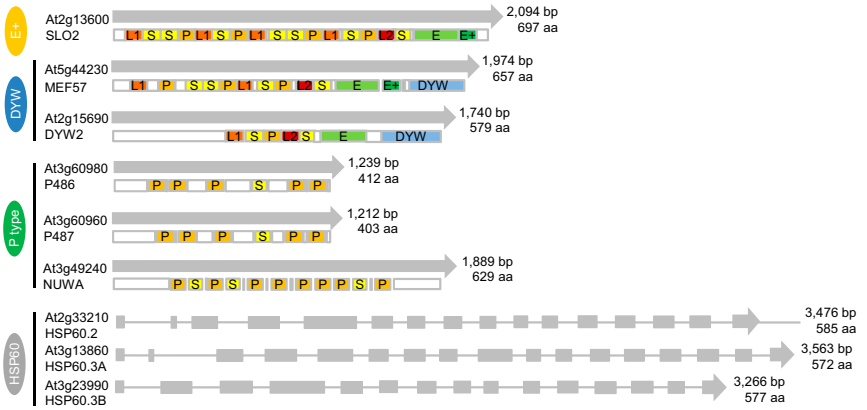

Fig. 1. Scheme of the primary structure of SLO2 and its interacting partners. The names/ID and locus codes and the type of PPR protein are indicated on the left, and the sizes in base pairs (bp) and amino acids (aa) on the right side of each scheme. The coding/exon fragments are indicated with gray boxes. The different PPR protein motifs (13, 37) are indicated with colors and capital letters (L1, brown; L2, red; S, yellow; P, orange; E, light green; E^+, dark green; and DYW, blue).

(NUWA-At3g49240, P486-At3g60980, and P487-At3g60960), and mtHSP60 chaperones (HSP60.2-At2g33210, HSP60.3A-At3g13860, and HSP60.3B-At3g23990), considered to be part of the import apparatus specific to the mitochondrial matrix (11) (Fig. 1). The limited number of PPR motifs in the DYW2 protein (Fig. 1), is likely to be insufficient for specific recognition of target RNAs and is reminiscent of the DYW1 protein in chloroplast (4).

Several SLO2 Interacting Partners Are Uniquely Localized in Mitochondria; Others Are Dual Localized in Mitochondria and Chloroplasts. As SLO2 is localized in mitochondria (10), its interactors are also expected to show mitochondrial localization. All of the SLO2 interacting partners were predicted to be localized in mitochondria by the SUBAcon program (12), except MEF57, predicted to be in plastids. For DYW2 and NUWA, proteomic data and reporter studies indicated dual targeting to mitochondria and chloroplasts (7, 8). NUWA mitochondrial localization was confirmed in *Arabidopsis* transgenic seedlings under the native promoter (13). In Fig. S2*A*, we show that the GFP signal of all GFP-tagged SLO2 candidate interactors consistently colocalized with the mitochondrial marker mitotracker/mt-rb in *Nicotiana* leaves, corroborating their mitochondrial localization, including for MEF57. In addition, a remarkably strong signal of NUWA-GFP was more frequently detected in chloroplasts (Fig. S2*B*) than in mitochondria. Likewise, DYW2-GFP showed strong chloroplast signals in several cells, in a dotted pattern (Fig. S2*B*), supporting dual localization for both proteins. The background signal at high laser gain, including chloroplast autofluorescence, is shown in Fig. S3*A*. HSP60 proteins, apart from the mitochondrial signal, also exhibited a signal associated with the cytosol (Fig. S2*A*).

SLO2 and Its Binding Partners Interact in Vivo with HSP60 Import Factors in Mitochondria. The suggested interaction between SLO2 and the mtHSP60 chaperones (Fig. S1), motivated us not only to confirm that these interactions occur in vivo in mitochondria, but also to check a possible interaction between the SLO2 binding PPR proteins and mtHSP60 import factors. All interactions were tested by bimolecular fluorescence complementation (BiFC). Both potential protein partners were tagged with the respective halves of the split-yellow fluorescent protein (YFP) protein and coinfiltrated pairwise in *Nicotiana* leaves. As summarized in Fig. 2*A*, the YFP signal was recovered when combining SLO2 or the selected PPR proteins with each of the mtHSP60 proteins, corroborating their interaction. No signal was recovered when combining them with ABERRANT PEROXISOME MORPHOLOGY 9 (APEM9) protein (14) (Fig. 2*A* and Fig. S3). The recovered YFP signal colocalized with the signal of the mitotracker/mt-rb mitochondrial marker (Fig. S4), proving that the interactions occur in mitochondria. To further substantiate the interaction of SLO2 and its binding PPR partners with the HSP60 chaperones, we coimmunoprecipitated human influenza hemagglutinin (HA)-/GFP-tagged SLO2, DYW2, or NUWA proteins together with GFP-/HA-tagged HSP60.2 and HSP60.3B proteins. Fig. 2*B* shows that HSP60.2 and HSP60.3B immunoprecipitated together with SLO2, DYW2, or NUWA, whereas APEM9 did not (Fig. S5*A*). Taken together, these results support the protein interaction of SLO2, DYW2, and NUWA with HSP60.2 and HSP60.3B in mitochondria.

A

		E+	DYW		P type				
		SLO2	MEF57	DYW2	P486	P487	NUWA	APEM9	PEX6
HSP60	HSP60.2	Strong	Strong	Strong	Strong	Strong	Strong	No	n.c.
	HSP60.3A	Strong	Strong	Strong	Strong	Strong	Strong	No	n.c.
	HSP60.3B	Strong	Strong	Strong	Strong	Strong	Strong	No	n.c.
	APEM9	No	No	No	No	No	No	n.c.	Strong

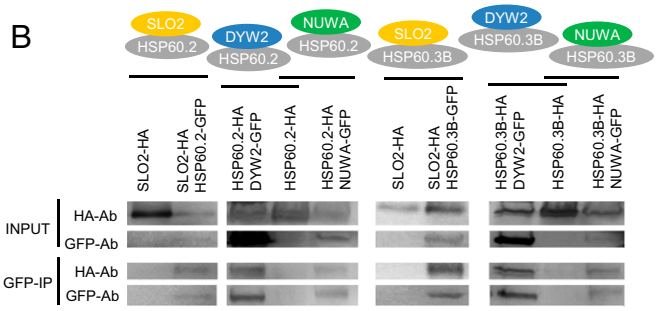

Fig. 2. Protein interaction of SLO2 and its partners MEF57, DYW2, P486, P487, and NUWA with mtHSP60 import factors. (*A*) Summary of the protein interactions between SLO2 or its partners and the HSP60 import factors in mitochondria, detected by BiFC assay in Figs. S3 *B–D* and S4. "Strong" and "weak" indicate the strength of the interactions according to the signal intensity under similar conditions. No, no interaction; n.c., not checked. (*B*) Total protein extracts (input) and GFP-immunoprecipitated proteins (GFP-IP) from *N. benthamiana* leaves infiltrated with SLO2-HA or HSP60.2-/HSP60.3B-HA together with HSP60.2-/HSP60.3B-GFP or DYW2-/NUWA-GFP constructs, 3 d after infiltration, analyzed by Western blot with anti-HA and anti-GFP antibodies (HA-Ab and GFP-Ab). *N. benthamiana* leaves infiltrated with the corresponding HA-tag constructs alone were taken as negative controls of the immunoprecipitation. Representative blots of at least two independent experiments for each combination are shown. Blots were cropped to the bands of interest (full-length blots in Fig. S5*B*). The contrast/brightness was adjusted for good visualization.

SLO2 Interacts in Vivo with DYW2 and NUWA Proteins in Mitochondria. Next we verified by BiFC whether the interaction of SLO2 with the P- and DYW-type PPR proteins detected by immunoprecipitation occurs in mitochondria. As presented in Fig. 3*A*, the recovery of the YFP signal when combining SLO2 with each PPR protein, confirmed the physical interaction of SLO2 with all of the tested PPR proteins. The colocalization of the recovered YFP signal with the mitotracker/mt-rb mitochondrial marker (Fig. S6*A*) certified that the interaction takes place in mitochondria. However, the recovery of the YFP signal was observed with a low frequency (less than 10% of the cells) and low intensity, except when combining SLO2 with NUWA (Fig. 3*A* and Fig. S6*A*). Because BiFC analyses tend to also detect rather weak and transient interactions, to corroborate the stable interaction between SLO2 and the DYW proteins or the P-type PPR protein NUWA, we coimmunoprecipitated tagged DYW proteins (MEF57-GFP and DYW2-GFP) and P-type PPR protein (NUWA-HA), together with tagged SLO2 (SLO2-HA or SLO2-GFP). As shown in Fig. 3*B* and Fig. S5*A*, SLO2 was immunoprecipitated together with all of the candidates tested, except with MEF57 and APEM9 control. These results endorse the specific interaction of SLO2 with all of the candidates tested, except for MEF57.

NUWA Enhances the Interaction Between SLO2 and DYW2 in Mitochondria in Vivo. Because some HSPs have been described to enhance mRNA or protein stability (15–17), we investigated whether the three SLO2 associated HSP60 proteins, interacting also with both DYW proteins (Fig. 2*A*), could stabilize the DYW proteins or the SLO2/DYW complexes, directly or through binding their target RNAs. Such stabilization could result in an increased interaction signal between SLO2 and the DYW proteins. To this end, we tested the interaction by BiFC in the presence and absence of the HSP60 partners (HSP60-HA), in parallel experiments, in different halves of the same *Nicotiana* leaf. The addition of HSP60 chaperones did not result in an increased interaction signal (Fig. S6*A*).

P-type PPR proteins also have been described to possess RNA or complex stabilization properties (2). Therefore, we checked whether the addition of the P-type PPR proteins detected as SLO2-interacting partners could improve the interaction between SLO2 and the DYW proteins. Interestingly, a clear increase in the SLO2 interaction with DYW2, appreciated by a high frequency (in around 90% of the cells) and intensity of the recovered YFP signal in parallel experiments, was detected in mitochondria in the presence of the P-type PPR protein NUWA (NUWA-HA) (Fig. 3 *A* and *C* and Fig. S6*A*), whereas coexpression of the other two P-type PPR proteins did not enhance the interaction (Fig. S6*A*). The increase in the interaction of SLO2 with DYW2 in the presence of NUWA (NUWA-His) was corroborated by coimmunoprecipitation (Fig. 3*B*), as reflected by a more intense SLO2-HA signal in the GFP immunoprecipitate (GFP-IP) compared with the input signal. The addition of NUWA, on the other hand, did not result in an enhanced signal for the SLO2/MEF57 interaction (Fig. 3 *A* and *C* and Fig. S6*A*).

DYW2 and NUWA Proteins Interact in Mitochondria and Chloroplasts. To elucidate whether the specific enhancement of the SLO2/DYW2 interaction by NUWA was conferred through their direct protein interactions, we compared affinities between each P-type PPR protein and the two DYW-type PPR proteins by BiFC assay. Although all three P-type PPR proteins could interact with both DYW-type PPR proteins in mitochondria, NUWA showed significantly stronger BiFC signal than the other two P-type PPR proteins (Fig. 3*A* and Fig. S6*B*). Interestingly, the interaction between NUWA and DYW2 took place mainly in mitochondria but, in some cells, the signal was detected in chloroplasts (Fig. S6*B*). This result is in agreement with the identification of NUWA and DYW2 as interactors of the chloroplastic E^+-type PPR CLB19 (18). Furthermore, the interaction between NUWA and DYW2 proteins was corroborated by coimmunoprecipitation (Fig. 3*B* and Fig. S5*A*).

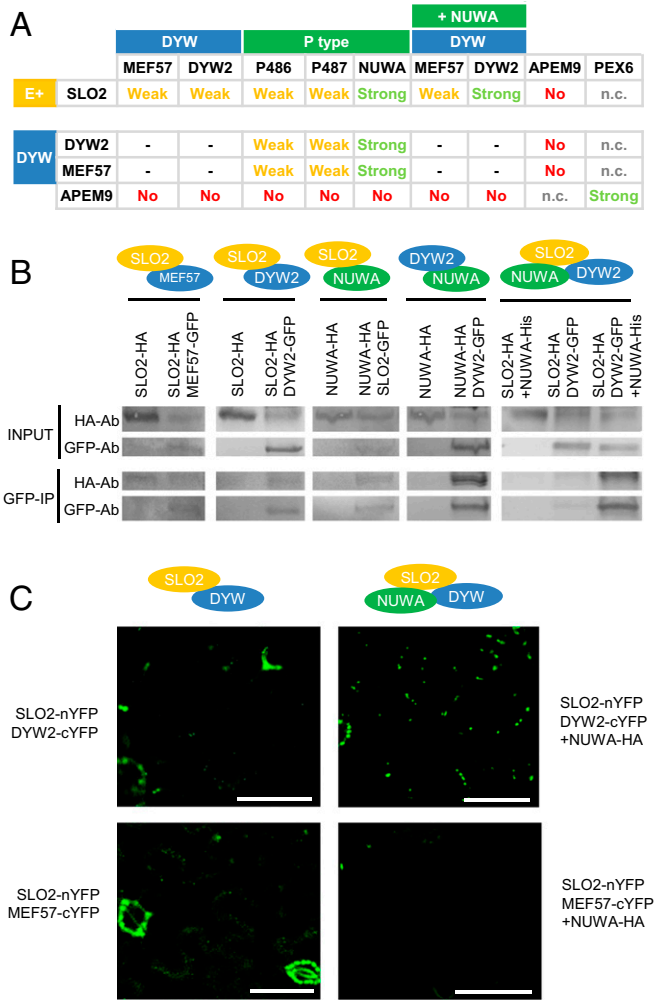

Fig. 3. Protein interaction between SLO2 and its PPR interacting partners MEF57, DYW2, P486, P487, and NUWA. (*A*) Summary of the protein interactions between SLO2, its DYW- and P-type PPR partners in mitochondria, detected by BiFC assay in Figs. S3 *B–D* and S6, as indicated in Fig. 2*A*. (*B*) Total protein extracts (input) and GFP-immunoprecipitated proteins (GFP-IP) from *N. benthamiana* leaves infiltrated with SLO2-HA together with MEF57-/DYW2-GFP, or NUWA-HA together with SLO2-/DYW2-GFP, or infiltrated with SLO2-HA together with DYW2-GFP or NUWA-His, or the combination of the three constructs. Proteins were extracted 3 d after infiltration and analyzed by Western blot as indicated in Fig. 2*B* (full-length blots in Fig. S5*B*). (*C*) *N. benthamiana* leaves infiltrated with SLO2-nYFP together with MEF57-/DYW2-cYFP, in the absence or presence of NUWA-HA construct, analyzed by confocal microscopy 3–6 d after infiltration. Green fluorescence is indicative of the localization of the reconstituted whole YFP protein (protein interaction). Representative individual cells of at least three independent experiments are shown. Single cells were cropped from the original image. (Scale bar, 50 μm.) Images for combinations without NUWA-HA (*Left*), with really low fluorescent signal, were taken at a higher laser gain condition, whereas the images where NUWA-HA was added (*Right*) were taken under lower gain conditions. For a proper comparison between proteins, images for both DYW2 and MEF57 proteins were taken under the same conditions. Images were extracted from Fig. S6*A*.

DYW2 and NUWA Proteins Form Homomers. We further investigated the capacity of SLO2 and its interacting PPR partners to homomerize by BiFC assay. Only the PPR proteins DYW2 and NUWA showed the capacity to form homomers (Fig. 4). Moreover, whereas NUWA homodimers were formed in both mitochondria

and chloroplasts, DYW2 homomerization was restricted to chloroplasts (Fig. 4).

DYW2 Is Involved in the Editing of the E$^+$-Type PPR Edited Sites. Finally, to clarify the biological relevance of the SLO2/DYW2 interaction, because we could not analyze homozygous *dyw2* knockout lines due to their embryo lethality (18), we generated *Arabidopsis* plants overexpressing the GFP-tagged DYW2 gene (Fig. S7). Two independent lines, containing at least fourfold higher levels of DYW2/DYW2-GFP transcripts than the DYW2 transcripts in wild type (Fig. S7*A*), were isolated. They showed a slow growth phenotype (Fig. 5 *A* and *B*), reminiscent of other PPR loss-of-function mutants. Editing analysis revealed a high number of affected editing sites, mainly down-edited, and some completely (100%) affected (Dataset S1). In particular, the E$^+$-type PPR SLO2 edited sites (10), including one identified in this work (Fig. S8), were down-edited (Dataset S1). Interestingly, this down-editing was also the case for most of the sites described to be edited by other E$^+$-type PPR proteins, but only for a few ones edited by DYW- or E-type PPRs, both in mitochondria and chloroplasts (Fig. 5 *C* and *D*). This result suggests that DYW2-mediated editing events are basically linked to E$^+$-type PPR proteins. Interestingly, as shown in Fig. S7*B*, the *NUWA* expression levels were higher in these DYW2-GFP overexpressing (DYW2-GFP-OE) lines compared with the wild-type plants, indicative of coordinated regulation. The work of Guillaumot et al. (18) on *dyw2* and *nuwa* loss-of-function mutants (18) also revealed a clear editing defect in most of the E$^+$-type PPR edited sites, including the SLO2 sites, corroborating a predominant role of DYW2 and NUWA proteins in E$^+$-type PPR-associated editing. Moreover, some sites not described to be regulated by known PPR proteins were also altered in the DYW2-GFP-OE lines (Dataset S1). This result points toward a hub function for DYW2; however, further investigation will be needed to establish a clear connection between DYW2 and non-PPR editing factors. The knockout line of the other DYW-type PPR partner of SLO2, MEF57 (Fig. S9), shows RNA editing defect at the *nad9*-92 site (Fig. S8), but no alteration at the SLO2 edited sites.

Discussion

PPR Editing Complexes. To date, the interactions between PPR proteins were restricted to the chloroplastic PPR protein DYW1, which can function in *trans* with the E-type PPR protein CRR4 (4). In this paper, we present evidence for the interaction between three types of PPR proteins (E$^+$, DYW, and P type) in mitochondria (SLO2, DYW2, and NUWA) (Figs. 1 and 3). The high *NUWA* expression levels in the DYW2-GFP-OE lines (Fig. S7*B*) reinforces the idea that NUWA is required by DYW2 to form a functional editosome with other editing factors. In addition, the dual localization and interaction of the DYW2 and the NUWA partner proteins (Figs. S2 and S6) suggest a coordinated regulation of organellar editing, supported by the identification of NUWA and DYW2 as interactors of the chloroplastic E$^+$-type PPR protein CLB19 (18) and the broad effect of DYW2 in E$^+$-type PPR edited sites (Fig. 5) (18). Taken together, we propose that E$^+$-type PPR proteins target the specific RNA sites, whereas P-type PPR protein NUWA assists the interaction between the E$^+$ partner and DYW2. Based on the current evidence (5), we hypothesize that DYW2 would provide the editing catalytic domain, both in mitochondria and chloroplasts. A model for the proposed PPR editosome mechanism is shown in Fig. 6.

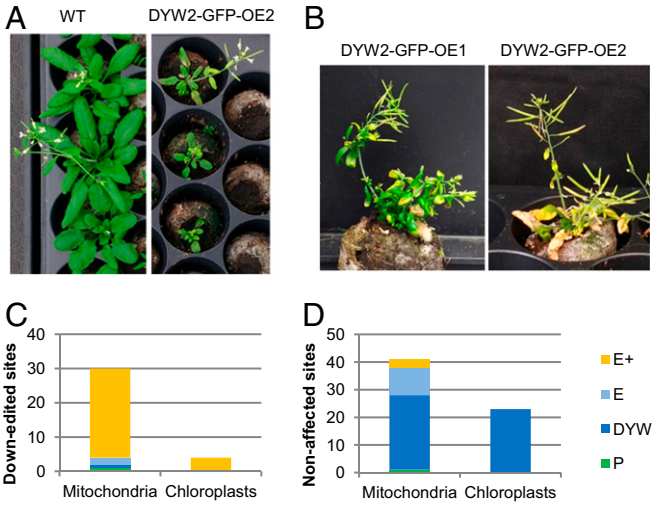

Fig. 5. Characterization of DYW2-GFP-OE lines. (*A* and *B*) Morphology of adult plants. Images of adult plants from the homozygous DYW2-GFP-OE2 line and the WT control, grown in parallel (*A*), and a detail of the morphology in two independent heterozygous DYW2-GFP-OE lines (*B*). Representative images of at least two independent experiments are shown. (*C* and *D*) RNA editing analysis of DYW2-GFP-OE lines. Editing analysis of rosette leaves from WT and two independent DYW2-GFP-OE lines are shown. Each independent line was analyzed once. The media and SD of the differences in editing percentage in both DYW2-GFP-OE lines with respect to the WT (Δ%) were calculated (Dataset S1). The number of sites modified by a particular type of PPR protein is represented. Both mitochondrial and chloroplastic sites are shown, split into down-edited (*C*) and nonaffected (*D*). A value of Δ% = 24% was taken as cutoff. The consistent data in both OE lines are shown. The list of PPR associated with editing sites was formed according to the literature (2, 20, 38) and this work.

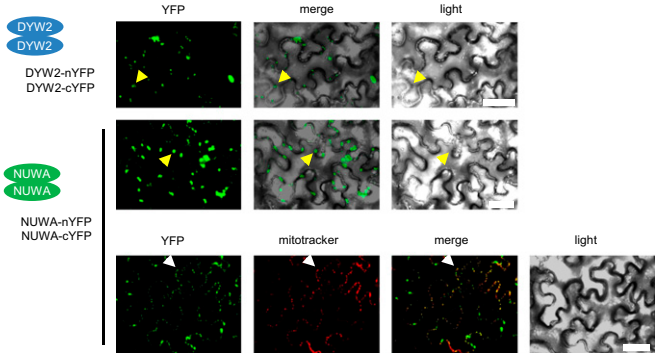

Fig. 4. Dimerization of DYW2 and NUWA. *N. benthamiana* leaves infiltrated with DYW2-/NUWA-nYFP together with DYW2-/NUWA-cYFP constructs and analyzed by confocal microscopy 3 d after infiltration. Green and red fluorescence are indicative of the localization of the reconstituted whole YFP protein (protein interaction) and the mitotracker mitochondrial marker, respectively. Representative individual cells of at least two independent experiments are shown, including their merged and light fields. Single cells were cropped from the original image. (Scale bar, 50 μm.) White arrows point to a mitochondrial signal dot and yellow arrows to a chloroplast signal. The contrast/brightness was adjusted for good visualization.

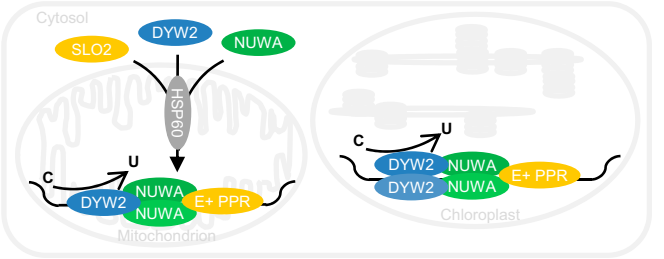

Fig. 6. Model of the tripartite PPR protein interaction in editosomes in mitochondria and chloroplasts.

Although the interaction between SLO2 and MEF57 detected by IP–MS could be confirmed by BiFC, it was not corroborated by coimmunoprecipitation (CoIP) (Fig. 3). The immunoprecipitation was realized from stable transgenic *Arabidopsis* plants, whereas the coimmunoprecipitation and BiFC assays were performed on transiently transformed *Nicotiana* leaves. These differences suggest the possibility that a factor present in *Arabidopsis* but not in *Nicotiana* could assist in the SLO2/MEF57 interaction. However, the possibility of absence of MEF57/SLO2 interaction would also be plausible. Indeed, the RNA editing analysis suggests that MEF57 protein is not required for the SLO2 editing ability (Fig. S8).

The observed down-editing effect in the DYW2-GFP-OE lines (Fig. 5 and Dataset S1) could likely be explained by a dominant negative effect of an inappropriate stoichiometry of the complex (19) or through capture of DYW2 interacting factors required by other editing complexes that target the same sites or by competition with other factors for the same editing sites (20–22). Furthermore, it was reported that the addition of a C-terminal tag to DYW proteins could inhibit their editing function (23, 24), while allowing interaction with other editing partners (4, 25–27). This might lead to a nonfunctional editosome, explaining the down-editing effect in these overexpressing lines. The observed DYW2-GFP-OE phenotype (Fig. 5) could be explained by the broad editing defect that would affect the organellar functions, impairing plant growth. This broad defect in the essential RNA editing process, would justify the lethality of the homozygous *dyw2* loss-of-function mutants (18).

Dual Localization of PPR Proteins. The PPR proteins DYW2 and NUWA have dual localization in both mitochondria and chloroplasts (Fig. S2). However, the protein characteristics and mechanisms responsible for this dual localization remain unclear. A significant number of proteins are dual targeted to both organelles via ambiguous targeting signals (28). It has been proposed that cytosolic chaperones may play a role in determining targeting specificity (29). In *Arabidopsis*, the mitochondrial HSP60 family has three members, considered to be part of the import apparatus specific to the mitochondrial matrix (30). We would expect that mutants of the interacting HSP60 proteins in this work affect RNA editing. However, if the three mtHSP60 proteins have any redundant function, a triple mutant would be needed to observe such editing defects.

PPR mRNA and Protein Complex Stabilization. The increased interaction of SLO2 and DYW2 when adding NUWA (Fig. 3) and the protein interaction of NUWA with both SLO2 and DYW2 (Fig. 3) suggest a possible scaffold or complex stabilization role of NUWA for the interaction between SLO2 and DYW2 in the editosome. In this context, a non-PPR editing factor (MORF8) was described to assist the interaction between an E^+-type PPR protein (MEF13) and another non-PPR factor (MORF3) (31). The fact that the P-type PPR protein NUWA assists in the interaction between an E^+ (SLO2) and a DYW (DYW2) protein, could reflect a more general mode of action of PPR proteins, hence representing the key for the discovery of similar tripartite PPR interactions and shedding light on the complex PPR editosome formation and action mechanisms.

Our results suggest that HSP60 proteins do not participate in the protein complex stabilization (Fig. S6*A*). They may assist in mitochondrial import of the partner proteins, as previously mentioned, or support RNA binding of the editing complexes. The chaperone HSP60 was suggested to have a highly specific nucleic acid-binding activity, presumably implicated in mtDNA stability (32). In protozoa, it has been demonstrated that a chaperone activity in the editosome increases the flexibility of U residues in the pre-mRNAs to facilitate the binding of gRNAs (33), providing a rational explanation for the U specificity of the editing reaction. P-type PPR subfamily members can also bind to specific RNA sequences (2), protecting the RNA from endonucleases and/or modifying its secondary structure to recruit general factors involved in RNA maturation. In this context, it will be interesting to check RNA binding activity of the HSP60 and P-type PPR proteins detected in this work.

Further investigation will be needed to understand the precise function of SLO2, DYW2, NUWA, and the HSP60 proteins in the SLO2 editosome complex and beyond.

Materials and Methods

IP–MS Assay. The IP–MS assay was performed as previously described (34), without modifications. Three biological replicates were used for each line.

BiFC. The predicted subcellular localization was analyzed by SUBAcon and SUBA3 programs (12, 35). For experimental subcellular localization and BiFC, the corresponding binary vectors were introduced into *Agrobacterium tumefaciens* strain GV3101. *Agrobacterium* was used to transiently transform young leaves of *Nicotiana benthamiana* grown on soil under long day conditions. For details, see *SI Materials and Methods*.

CoIP. A modified μMACS Epitope Tag Protein Isolation Kit (Miltenyi) protocol (34) was followed. For details, see *SI Materials and Methods*.

T-DNA Insertion, Complemented, and Overexpressing Lines. *Arabidopsis thaliana* T-DNA insertion mutant line N585176 from the SALK collection was used and complemented with the *35S::MEF57-GFP* construct. The DYW2-GFP-OE lines were generated transforming Col-0 *A. thaliana* plants with the *35S::DYW2-GFP* construct.

RNA Editing Analysis. Specific cDNAs were generated as described previously (36). The sequence data for each gene-specific RT-PCR product were obtained commercially and compared for analysis (Macrogen). Ratios between heights of C and T signals were calculated with the DNADynamo software (BlueTractorSoftware). The *Arabidopsis slo2-2*, *slo2-3*, complemented *slo2-2*, and complemented *slo2-3* lines were taken from our previous work (10).

A detailed description of the plasmid construction and full methods are described in *SI Materials and Methods*.

Data Availability. All data generated or analyzed during this study are included in this article (and *Supporting Information*).

ACKNOWLEDGMENTS. N.A.-C. and D.V.D.S. thank Maria Helena de Souza Goldman for the *N. benthamiana* seeds and helpful suggestions regarding experimental design and data interpretation; Irina Vaseva for critical reading of the first draft of this manuscript; and Yordanka Yordanova for experimental help in genotyping the *mef57* mutant line. D.V.D.S. acknowledges the Research Foundation Flanders for financial support (Project G.0C84.14N). B.D.R. was funded by a Marie Curie long-term postdoctoral fellowship (FP7-PEOPLE-2009-IEF-252503) and by The Netherlands Organization for Scientific Research (NWO; VIDI-864.13.001). D.W. acknowledges funding by NWO (ERA-CAPS Project EURO-PEC; 849.13.006). M.T. was supported by Deutsche Forschungsgemeinschaft Grants TA624/4-2, TA624/-1, and TA624/10-1.

1. Barkan A, Small I (2014) Pentatricopeptide repeat proteins in plants. *Annu Rev Plant Biol* 65:415–442.
2. Shikanai T (2015) RNA editing in plants: Machinery and flexibility of site recognition. *Biochim Biophys Acta* 1847:779–785.
3. Leu KC, Hsieh MH, Wang HJ, Hsieh HL, Jauh GY (2016) Distinct role of Arabidopsis mitochondrial P-type pentatricopeptide repeat protein-modulating editing protein, PPME, in nad1 RNA editing. *RNA Biol* 13:593–604.
4. Boussardon C, et al. (2012) Two interacting proteins are necessary for the editing of the NdhD-1 site in Arabidopsis plastids. *Plant Cell* 24:3684–3694.
5. Sun T, Bentolila S, Hanson MR (2016) The unexpected diversity of plant organelle RNA editosomes. *Trends Plant Sci* 21:962–973.
6. Yin P, et al. (2013) Structural basis for the modular recognition of single-stranded RNA by PPR proteins. *Nature* 504:168–171.
7. Colcombet J, et al. (2013) Systematic study of subcellular localization of Arabidopsis PPR proteins confirms a massive targeting to organelles. *RNA Biol* 10:1557–1575.
8. Hooper CM, Castleden IR, Tanz SK, Aryamanesh N, Millar AH (2017) SUBA4: The interactive data analysis centre for Arabidopsis subcellular protein locations. *Nucleic Acids Res* 45:D1064–D1074.

9. Law YS, et al. (2015) Phosphorylation and dephosphorylation of the presequence of precursor MULTIPLE ORGANELLAR RNA EDITING FACTOR3 during import into mitochondria from Arabidopsis. *Plant Physiol* 169:1344–1355.
10. Zhu Q, et al. (2012) SLO2, a mitochondrial pentatricopeptide repeat protein affecting several RNA editing sites, is required for energy metabolism. *Plant J* 71:836–849.
11. Murcha MW, et al. (2014) Protein import into plant mitochondria: Signals, machinery, processing, and regulation. *J Exp Bot* 65:6301–6335.
12. Hooper CM, et al. (2014) SUBAcon: A consensus algorithm for unifying the subcellular localization data of the Arabidopsis proteome. *Bioinformatics* 30:3356–3364.
13. He S, et al. (2017) A novel imprinted gene NUWA controls mitochondrial function in early seed development in Arabidopsis. *PLoS Genet* 13:e1006553.
14. Goto S, Mano S, Nakamori C, Nishimura M (2011) Arabidopsis ABERRANT PEROXISOME MORPHOLOGY9 is a peroxin that recruits the PEX1-PEX6 complex to peroxisomes. *Plant Cell* 23:1573–1587.
15. Bender T, Lewrenz I, Franken S, Baitzel C, Voos W (2011) Mitochondrial enzymes are protected from stress-induced aggregation by mitochondrial chaperones and the Pim1/LON protease. *Mol Biol Cell* 22:541–554.
16. Kim KH, et al. (2012) Rescue of PINK1 protein null-specific mitochondrial complex IV deficits by ginsenoside Re activation of nitric oxide signaling. *J Biol Chem* 287:44109–44120.
17. Wang R, et al. (2016) HSP90 regulates temperature-dependent seedling growth in Arabidopsis by stabilizing the auxin co-receptor F-box protein TIR1. *Nat Commun* 7:10269.
18. Guillaumot D, et al. (2017) Two interacting PPR proteins are major *Arabidopsis* editing factors in plastid and mitochondria. *Proc Natl Acad Sci USA* 114:8877–8882.
19. Veitia RA (2007) Exploring the molecular etiology of dominant-negative mutations. *Plant Cell* 19:3843–3851.
20. Bentolila S, Knight W, Hanson M (2010) Natural variation in Arabidopsis leads to the identification of REME1, a pentatricopeptide repeat-DYW protein controlling the editing of mitochondrial transcripts. *Plant Physiol* 154:1966–1982.
21. Blanc V, et al. (2001) Identification of GRY-RBP as an apolipoprotein B RNA-binding protein that interacts with both apobec-1 and apobec-1 complementation factor to modulate C to U editing. *J Biol Chem* 276:10272–10283.
22. Hayes ML, Giang K, Berhane B, Mulligan RM (2013) Identification of two pentatricopeptide repeat genes required for RNA editing and zinc binding by C-terminal cytidine deaminase-like domains. *J Biol Chem* 288:36519–36529.
23. Wagoner JA, Sun T, Lin L, Hanson MR (2015) Cytidine deaminase motifs within the DYW domain of two pentatricopeptide repeat-containing proteins are required for site-specific chloroplast RNA editing. *J Biol Chem* 290:2957–2968.
24. Zehrmann A, Verbitskiy D, Härtel B, Brennicke A, Takenaka M (2010) RNA editing competence of trans-factor MEF1 is modulated by ecotype-specific differences but requires the DYW domain. *FEBS Lett* 584:4181–4186.
25. Bentolila S, et al. (2012) RIP1, a member of an Arabidopsis protein family, interacts with the protein RARE1 and broadly affects RNA editing. *Proc Natl Acad Sci USA* 109:E1453–E1461.
26. Sun T, et al. (2013) An RNA recognition motif-containing protein is required for plastid RNA editing in Arabidopsis and maize. *Proc Natl Acad Sci USA* 110:E1169–E1178.
27. Takenaka M, et al. (2012) Multiple organellar RNA editing factor (MORF) family proteins are required for RNA editing in mitochondria and plastids of plants. *Proc Natl Acad Sci USA* 109:5104–5109.
28. Carrie C, et al. (2009) Approaches to defining dual-targeted proteins in Arabidopsis. *Plant J* 57:1128–1139.
29. Kriechbaumer V, von Löffelholz O, Abell BM (2012) Chaperone receptors: Guiding proteins to intracellular compartments. *Protoplasma* 249:21–30.
30. Murcha MW, Narsai R, Devenish J, Kubiszewski-Jakubiak S, Whelan J (2015) MPIC: A mitochondrial protein import components database for plant and non-plant species. *Plant Cell Physiol* 56:e10.
31. Glass F, Härtel B, Zehrmann A, Verbitskiy D, Takenaka M (2015) MEF13 requires MORF3 and MORF8 for RNA editing at eight targets in mitochondrial mRNAs in Arabidopsis thaliana. *Mol Plant* 8:1466–1477.
32. Kaufman BA, et al. (2000) In organello formaldehyde crosslinking of proteins to mtDNA: Identification of bifunctional proteins. *Proc Natl Acad Sci USA* 97:7772–7777.
33. Leeder WM, Voigt C, Brecht M, Göringer HU (2016) The RNA chaperone activity of the Trypanosoma brucei editosome raises the dynamic of bound pre-mRNAs. *Sci Rep* 6: 19309.
34. Wendrich JR, Boeren S, Möller BK, Weijers D, De Rybel B (2017) In vivo identification of plant protein complexes using IP-MS/MS. *Methods Mol Biol* 1497:147–158.
35. Tanz SK, et al. (2013) SUBA3: A database for integrating experimentation and prediction to define the SUBcellular location of proteins in Arabidopsis. *Nucleic Acids Res* 41:D1185–D1191.
36. Takenaka M, Brennicke A (2007) RNA editing in plant mitochondria: Assays and biochemical approaches. *Methods Enzymol* 424:439–458.
37. Lurin C, et al. (2004) Genome-wide analysis of Arabidopsis pentatricopeptide repeat proteins reveals their essential role in organelle biogenesis. *Plant Cell* 16:2089–2103.
38. Sun T, et al. (2015) A zinc finger motif-containing protein is essential for chloroplast RNA editing. *PLoS Genet* 11:e1005028.
39. Tanaka Y, et al. (2012) Gateway vectors for plant genetic engineering: Overview of plant vectors, application for bimolecular fluorescence complementation (BiFC) and multigene construction genetic engineering. *Basics, New Applications and Responsibilities* (InTech, Croatia), pp 35–68.
40. Nakagawa T, et al. (2007) Improved Gateway binary vectors: High-performance vectors for creation of fusion constructs in transgenic analysis of plants. *Biosci Biotechnol Biochem* 71:2095–2100.
41. Nelson BK, Cai X, Nebenführ A (2007) A multicolored set of in vivo organelle markers for co-localization studies in Arabidopsis and other plants. *Plant J* 51:1126–1136.
42. Mohammadzadeh S, et al. (2016) Co-expression of hepatitis C virus polytope–HBsAg and p19-silencing suppressor protein in tobacco leaves. *Pharm Biol* 54:465–473.
43. Clough SJ, Bent AF (1998) Floral dip: A simplified method for Agrobacterium-mediated transformation of Arabidopsis thaliana. *Plant J* 16:735–743.
44. Sparkes IA, Hawes C, Baker A (2005) AtPEX2 and AtPEX10 are targeted to peroxisomes independently of known endoplasmic reticulum trafficking routes. *Plant Physiol* 139: 690–700.